

Antishadowing effects in the unitarized BFKL equation

Jianhong Ruan, Zhenqi Shen, Jifeng Yang and Wei Zhu*

Department of Physics, East China Normal University, Shanghai 200062, P.R. China

Abstract

A unitarized BFKL equation incorporating shadowing and antishadowing corrections of the gluon recombination is proposed. This equation reduces to the Balitsky-Kovchegov evolution equation near the saturation limit. We find that the antishadowing effects have a sizeable influence on the gluon distribution function in the preasymptotic regime.

PACS numbers: 13.60.Hb; 12.38.Bx.

keywords: antishadowing; evolution equation; QCD recombination process

arXiv:hep-ph/0608028v2 13 Nov 2006

*Corresponding author, E-mail: weizhu@mail.ecnu.edu.cn

1 Introduction

The growth of cross sections with gluon splitting according to the DGLAP [1] and BFKL [2] evolution equations would violate the unitarity. Therefore, the corrections of the higher order QCD, which shadow the growth of parton densities and lead to an eventual saturation of parton densities, become a focus of intensive study in recent years. In this respect, the GLR-MQ (by Gribov, Levin Ryskin in [3] and Mueller and Qiu in [4]) and BK (by Balitsky and Kovchegov in [5]) equations are broadly regarded as two solvable models to compute the shadowing corrections to the DGLAP and BFKL equations, respectively.

One of the key problems in restoring unitarity is the origin of the negative corrections. In the viewpoint of elementary QCD interaction, the suppression of the gluon splitting comes from its inverse process—the gluon recombination. The negative screening effects in the recombination processes originally occur in the interferant cut-diagrams of the recombination amplitudes [3,6]. For computing the contributions from the interference processes, the AGK cutting rules [7] were used in the derivation of the GLR-MQ equation.

On the other hand, one of us (Zhu) disputed the above mentioned applications of the AGK cutting rules in the GLR-MQ equation, and used the TOPT-cutting rules based on the time ordered perturbation theory (TOPT) instead of the AGK cutting rules to expose the relations among various cut diagrams in a recombination process [6]. Thus, we can completely compute the contributions of the gluon recombination processes. Consequently, a modified DGLAP equation was proposed [6,8]. A remarkable property of this equation is that the positive antishadowing and negative shadowing components in the nonlinear evolution equation are naturally separated. As a result, the corrections from gluon recombination at small x depend not only on the size of gluon density at this value of x , but also on the shape of gluon density in the region $[x/2, x]$. Thus, the shadowing effects in the evolution process will be weakened by the antishadowing effects if the gluon

distribution has a steeper form.

The antishadowing effects always coexist with the shadowing effects in the QCD recombination processes as a general conclusion of the momentum conservation [9]. Therefore, similar antishadowing effects should exist in any unitarized BFKL equation. In this work we try to find the antishadowing effects in the unitarized BFKL equation. The total momentum carried by gluons is not changed as a result of the gluon fusion but simply redistributed to different x regions. The depleted momentum due to the fusion is heaped up step by step toward a larger x direction, which leads to an enhanced density of higher momentum gluons (i.e. the antishadowing effects). We shall show that the antishadowing effects have a sizeable influence on the gluon distribution function in the preasymptotic regime.

The paper is organized as follows. In Section 2 we derive a unitarized BFKL equation with the gluon recombination, which contains the contributions of the shadowing and antishadowing effects. The numerical analysis of our equation are presented in Section 3. In Section 4 we show that our equation reduces to the BK equation near the saturation limit. We also compare our equation with a modified BK equation in this Section.

2 The evolution equation incorporating shadowing and antishadowing effects

We develop a unified framework to construct the evolution equations for both the integrated and unintegrated gluon distribution functions. We begin from a deep inelastic scattering process, where the unintegrated gluon distribution is measured. In the k_T -factorization scheme, the cross section is decomposed into

$$\begin{aligned}
 & d\sigma(\text{probe}^*P \rightarrow k'X) \\
 &= f(x_1, \underline{k}_1^2) \otimes \mathcal{K}\left(\frac{\underline{k}^2}{\underline{k}_1^2}, \frac{x}{x_1}, \alpha_s\right) \otimes d\sigma(\text{probe}^*k \rightarrow k') \\
 &\equiv \Delta f(x, \underline{k}^2) \otimes d\sigma(\text{probe}^*k \rightarrow k'), \tag{1}
 \end{aligned}$$

which contains the perturbative evolution kernel \mathcal{K} , the nonperturbative unintegrated gluon distribution function f and the probe^* -parton cross section $d\sigma(\text{probe}^*k \rightarrow k')$. For simplicity, we take the fixed QCD coupling in this work. According to the scale-invariant parton picture of the renormalization group [10], we regard $\Delta f(x, \underline{k}^2)$ as the increment of the distribution $f(x_1, \underline{k}_1^2)$ when it evolves from (x_1, \underline{k}_1^2) to (x, \underline{k}^2) . Thus, the connection between the two functions $f(x_1, \underline{k}_1^2)$ and $f(x, \underline{k}^2)$ via Eq.(1) is

$$\begin{aligned}
 & f(x, \underline{k}^2) = f(x_1, \underline{k}_1^2) + \Delta f(x, \underline{k}^2) \\
 &= f(x_1, \underline{k}_1^2) + \int_{\underline{k}_1^2}^{\underline{k}^2} \frac{d\underline{k}_1^2}{\underline{k}_1^2} \int_x^1 \frac{dx_1}{x_1} \mathcal{K}\left(\frac{\underline{k}^2}{\underline{k}_1^2}, \frac{x}{x_1}, \alpha_s\right) f(x_1, \underline{k}_1^2), \tag{2}
 \end{aligned}$$

The relation of the unintegrated gluon distribution with the integrated gluon distribution is

$$G(x, Q^2) \equiv xg(x, Q^2) = \int_{\underline{k}_{min}^2}^{Q^2} \frac{d\underline{k}^2}{\underline{k}^2} x f(x, \underline{k}^2) \equiv \int_{\underline{k}_{min}^2}^{Q^2} \frac{d\underline{k}^2}{\underline{k}^2} F(x, \underline{k}^2), \tag{3}$$

or

$$f(x, \underline{k}^2) = Q^2 \frac{\partial g(x, Q^2)}{\partial Q^2} \Big|_{Q^2 = \underline{k}^2}. \quad (4)$$

In the evolution along the transverse momentum (or along the longitudinal momentum), we differentiate Eq.(2) with respect to \underline{k}^2 (or to x) and get

$$\begin{aligned} & \frac{\partial f(x, \underline{k}^2)}{\partial \underline{k}^2} \\ &= \int_x^1 \frac{dx_1}{x_1} \frac{1}{\underline{k}_1^2} \mathcal{K} \left(\frac{\underline{k}^2}{\underline{k}_1^2}, \frac{x}{x_1}, \alpha_s \right) f(x_1, \underline{k}_1^2) \Big|_{\underline{k}_1^2 = \underline{k}^2} \\ &+ \int_{\underline{k}_{1min}^2}^{\underline{k}^2} \frac{d\underline{k}_1^2}{\underline{k}_1^2} \int_x^1 \frac{dx_1}{x_1} \frac{\partial \mathcal{K} \left(\frac{\underline{k}^2}{\underline{k}_1^2}, \frac{x}{x_1}, \alpha_s \right)}{\partial \underline{k}^2} f(x_1, \underline{k}_1^2), \end{aligned} \quad (5)$$

or

$$\begin{aligned} & - \frac{\partial f(x, \underline{k}^2)}{\partial x} \\ &= \int_{\underline{k}_{1min}^2}^{\underline{k}^2} \frac{d\underline{k}_1^2}{\underline{k}_1^2} \frac{1}{x_1} \mathcal{K} \left(\frac{\underline{k}^2}{\underline{k}_1^2}, \frac{x}{x_1}, \alpha_s \right) f(x_1, \underline{k}_1^2) \Big|_{x_1 = x} \\ &- \int_{\underline{k}_{1min}^2}^{\underline{k}^2} \frac{d\underline{k}_1^2}{\underline{k}_1^2} \int_x^1 \frac{dx_1}{x_1} \frac{\partial \mathcal{K} \left(\frac{\underline{k}^2}{\underline{k}_1^2}, \frac{x}{x_1}, \alpha_s \right)}{\partial x} f(x_1, \underline{k}_1^2), \end{aligned} \quad (6)$$

respectively. Generally, the resummation solution is hard to obtain from these two equations. However, at the $LL(\underline{k}^2)A$ (or at the $LL(1/x)A$) the evolution kernel \mathcal{K} in Eq.(5) (or in Eq.(6)) is only the function of the longitudinal variable (or of the transverse variables) and the second term on the right-hand side of Eq.(5) (or of Eq.(6)) vanishes. In this case, the resummation becomes possible. For example, using Eq.(3) we write

$$\begin{aligned} \Delta g(x, Q^2) &\equiv \int_{\underline{k}_{min}^2}^{Q^2} \frac{d\underline{k}^2}{\underline{k}^2} \Delta f(x, \underline{k}^2) \\ &= \int_{\underline{k}_{min}^2}^{Q^2} \frac{d\underline{k}^2}{\underline{k}^2} \int_{\underline{k}_{1min}^2}^{\underline{k}^2} \frac{d\underline{k}_1^2}{\underline{k}_1^2} \int_x^1 \frac{dx_1}{x_1} \mathcal{K}_{DGLAP} \left(\frac{x}{x_1}, \alpha_s \right) f(x_1, \underline{k}_1^2) \\ &= \int_{\underline{k}_{min}^2}^{Q^2} \frac{d\underline{k}^2}{\underline{k}^2} \int_x^1 \frac{dx_1}{x_1} \mathcal{K}_{DGLAP} \left(\frac{x}{x_1}, \alpha_s \right) g(x_1, \underline{k}^2), \end{aligned} \quad (7)$$

and

$$g(x, Q^2) = g(x_1, \underline{k}^2) + \Delta g(x, Q^2). \quad (8)$$

On the other hand, at $DLL(Q^2)A$ we have

$$\mathcal{K}_{DGLAP} \frac{dx_1}{x_1} = \frac{\alpha_s N_c}{\pi} \frac{dx_1}{x}. \quad (9)$$

Thus, from Eqs.(5) and (7) one can get the DGLAP equation at small x for the gluon distribution

$$\begin{aligned} Q^2 \frac{\partial g(x, Q^2)}{\partial Q^2} &= \int_x^1 \frac{dx_1}{x_1} \mathcal{K}_{DGLAP} \left(\frac{x}{x_1}, \alpha_s \right) g(x_1, Q^2) \\ &= \frac{\alpha_s N_c}{\pi} \int_x^1 \frac{dx_1}{x_1} \frac{x_1}{x} g(x_1, Q^2). \end{aligned} \quad (10)$$

Now let us consider the corrections of the gluon recombination to the DGLAP equation. The one step evolution containing the gluon recombination is illustrated in Fig.1(a), where the initial gluons from the two legs are resummed using the DGLAP equation. Four different kinds of the evolution kernels for $\mathcal{K}_{MD-DGLAP}$ are listed in Fig.2. Similar to Eqs.(7) and (8) we derive the modified DGLAP equation from

$$\begin{aligned} G(x, Q^2) &= G(x_1, Q_1^2) + \Delta G(x, Q^2) \\ &= G(x_1, Q_1^2) - 2 \int_{Q_{1min}^2}^{Q^2} \frac{dQ_1^2}{Q_1^4} \int_x^{1/2} \frac{dx_1}{x_1} \frac{x}{x_1} \mathcal{K}_{MD-DGLAP} \left(\frac{x}{x_1}, \alpha_s \right) G^{(2)}(x_1, Q_1^2) \\ &\quad + \int_{Q_{1min}^2}^{Q^2} \frac{dQ_1^2}{Q_1^4} \int_{x/2}^{1/2} \frac{dx_1}{x_1} \frac{x}{x_1} \mathcal{K}_{MD-DGLAP} \left(\frac{x}{x_1}, \alpha_s \right) G^{(2)}(x_1, Q_1^2), \end{aligned} \quad (11)$$

where a power suppression factor $1/Q_1^2$ has been extracted from the evolution kernel. The positive and negative terms are from the contributions of the diagrams Fig.2(a) and (b), respectively. The TOPT calculations [8] give

$$\begin{aligned}
& \mathcal{K}^{MD-DGLAP} \frac{dx_1}{x_1} \\
= & \frac{\alpha_s^2}{8} \frac{N_c^2}{N_c^2 - 1} \frac{(2x_1 - x)(72x_1^4 - 48x_1^3x + 140x_1^2x^2 - 116x_1x^3 + 29x^4)}{x_1^5 x} dx_1 \\
& \xrightarrow{x \ll x_1} 18\alpha_s^2 \frac{N_c^2}{N_c^2 - 1} \frac{dx_1}{x}.
\end{aligned} \tag{12}$$

The gluon correlation function $G^{(2)}$ is a generalization of the gluon distribution beyond the leading twist. It is usually modelled as the product of two gluon distributions [6]. For example,

$$G^{(2)}(x, Q^2) = R_G G^2(x, Q^2), \tag{13}$$

where $R_G = 1/(\pi R^2)$ is a correlation coefficient with the dimension $[L^{-2}]$, R is the effective correlation length of two recombination gluons and we take $R = 5\text{GeV}^{-1}$ (the radius of a nucleon). Setting Eqs.(12) and (13) to Eq.(11), we obtain the modified DGLAP equation combining DGLAP dynamics at small x

$$\begin{aligned}
& \frac{\partial G(x, Q^2)}{\partial \ln Q^2} \\
= & \frac{\alpha_s N_c}{\pi} \int_x^1 \frac{dx_1}{x_1} G(x_1, Q^2) - \frac{36\alpha_s^2}{\pi Q^2 R^2} \frac{N_c^2}{N_c^2 - 1} \int_x^{1/2} \frac{dx_1}{x_1} G^2(x_1, Q^2) \\
& + \frac{18\alpha_s^2}{\pi Q^2 R^2} \frac{N_c^2}{N_c^2 - 1} \int_{x/2}^{1/2} \frac{dx_1}{x_1} G^2(x_1, Q^2) \\
= & \frac{\alpha_s N}{\pi} \int_x^1 \frac{dx_1}{x_1} G(x_1, Q^2) - \frac{18\alpha_s^2}{\pi Q^2 R^2} \frac{N_c^2}{N_c^2 - 1} \int_x^{1/2} \frac{dx_1}{x_1} G^2(x_1, Q^2) \\
& + \frac{18\alpha_s^2}{\pi Q^2 R^2} \frac{N_c^2}{N_c^2 - 1} \int_{x/2}^x \frac{dx_1}{x_1} G^2(x_1, Q^2).
\end{aligned} \tag{14}$$

It is interesting to compare this small- x version of the modified DGLAP equation with the GLR-MQ equation, which is [4]

$$\frac{\partial G(x, Q^2)}{\partial \ln Q^2}$$

$$= \frac{\alpha_s N_c}{\pi} \int_x^1 \frac{dx_1}{x_1} G(x_1, Q^2) - \frac{36\alpha_s^2}{8Q^2 R^2} \frac{N_c^2}{N_c^2 - 1} \int_x^{1/2} \frac{dx_1}{x_1} G^2(x_1, Q^2), \quad (15)$$

where

$$G^{(2)}(x, Q^2) = \frac{9}{8\pi R^2} G^2(x, Q^2), \quad (16)$$

is assumed. Although both of the two equations have been hoped to describe the corrections of the gluon recombination to the linear DGLAP equation at the *DLLA*, they have different forms due to the following reasons:

(1) The GLR-MQ equation is derived basing on the following two works. One is the idea that the negative shadowing effects arise from the interference processes of the gluon recombination. Gribov, Levin and Ryskin used the AGK cutting rules to show that the contributions from the real cut diagrams (see Fig.2(a)) and the interferant cut diagrams (see Fig.2(b)) only differ in the numerical weights, which is 2 and -4, respectively. Thus, the net effects of the gluon recombination can be simply calculated by multiplying the real diagrams by a negative weight. Obviously, the antishadowing effects in this approach are completely cancelled by the shadowing effects and the resulting evolution equation violates the momentum conservation. Another work is the calculation of the recombination functions at the *DLLA* in a covariant perturbation theory by Mueller and Qiu [4], where a special treatment was used to remove the infrared (IR) singularities in the gluonic twist-4 coefficient functions. The gluon recombination functions in the GLR-MQ equation are separated out from the above mentioned IR-safe coefficient functions.

(2) In the derivation of the modified DGLAP equation, the TOPT was first used to establish the relations among all the relevant cut diagrams in Fig.2 [6]. We showed that the shadowing and antishadowing effects share the same recombination function but occupy different kinematic regions. On the other hand, the contributions of the two virtual diagrams Fig.2(c) and (d) cancel against each other. Thus, the net effects depend

not only on the local value of the gluon distribution at the observed point, but also on the shape of the gluon distribution when the Bjorken variable goes from x to $x/2$. In consequence, the shadowing effects in the evolution process will be obviously weakened by the antishadowing effects if the distribution is steeper [11]. We found that the same TOPT framework allows us to calculate the recombination functions including quarks and gluons in the whole region of x at the $LL(Q^2)A$. Consequently, the momentum conservation is restored in the modified DGLAP equation [6]. We also showed in [8] that the gluon recombination functions can be reasonably separated from the twist-4 coefficient functions in the TOPT approach without the above mentioned special treatment, though the results of the two methods only differ by a constant at the $DLLA$.

In next step, we consider the recombination of two unintegrated gluon distribution functions, which obey the BFKL equation. The cut diagram corresponding to Fig.1(a) is Fig.1(b), where the dashed box implies a new recombination kernel of two BFKL solutions. The initial gluons couple with the gluonic dipole and it means that two initial legs evolve according to the BFKL dynamics. One can expect that $\mathcal{K}_{MD-BFKL}$ is more complicated than $\mathcal{K}_{MD-DGLAP}$. As an approximate model, we use kernel $\mathcal{K}_{MD-DGLAP}$ to replace the kernel $\mathcal{K}_{MD-BFKL}$ in Fig.1(b). In the concrete, the contributions of two correlated unintegrated distribution functions $F^{(2)}$ to the measured (integrated) distribution G via the recombination processes are

$$\begin{aligned} \Delta G(x, Q^2) = & -2 \int_{Q_{min}^2}^{Q^2} \frac{d\mathbf{k}^2}{\mathbf{k}^4} \int_x^{1/2} \frac{dx_1}{x_1} \frac{x}{x_1} \mathcal{K}_{MD-DGLAP} \left(\frac{x}{x_1}, \alpha_s \right) F^{(2)}(x_1, \mathbf{k}^2) \\ & + \int_{Q_{min}^2}^{Q^2} \frac{d\mathbf{k}^2}{\mathbf{k}^4} \int_{x/2}^{1/2} \frac{dx_1}{x_1} \frac{x}{x_1} \mathcal{K}_{MD-DGLAP} \left(\frac{x}{x_1}, \alpha_s \right) F^{(2)}(x_1, \mathbf{k}^2). \end{aligned} \quad (17)$$

Thus, we have

$$\begin{aligned}
\Delta F(x, \underline{k}^2) &= Q^2 \frac{\partial \Delta G(x, Q^2)}{\partial Q^2} \Big|_{Q^2=\underline{k}^2} \\
&= -\frac{2}{\underline{k}^2} \int_x^{1/2} \frac{dx_1}{x_1} \frac{x}{x_1} \mathcal{K}_{MD-DGLAP} \left(\frac{x}{x_1}, \alpha_s \right) F^{(2)}(x_1, \underline{k}^2) \\
&\quad + \frac{1}{\underline{k}^2} \int_{x/2}^{1/2} \frac{dx_1}{x_1} \frac{x}{x_1} \mathcal{K}_{MD-DGLAP} \left(\frac{x}{x_1}, \alpha_s \right) F^{(2)}(x_1, \underline{k}^2). \tag{18}
\end{aligned}$$

Using Eqs.(6) and (12) we obtain the corrections to the evolution of the unintegrated gluon distribution along small x direction

$$-x \frac{\partial F(x, \underline{k}^2)}{\partial x} = -36\alpha_s^2 \frac{N_c^2}{N_c^2 - 1} \frac{1}{\underline{k}^2} F^{(2)}(x, \underline{k}^2) + 18\alpha_s^2 \frac{N_c^2}{N_c^2 - 1} \frac{1}{\underline{k}^2} F^{(2)}\left(\frac{x}{2}, \underline{k}^2\right). \tag{19}$$

Combining with the BFKL equation, we obtain a unitarized BFKL equation

$$\begin{aligned}
& -x \frac{\partial F(x, \underline{k}^2)}{\partial x} \\
&= \frac{\alpha_s N_c \underline{k}^2}{\pi} \int_{\underline{k}'^2_{min}}^{\infty} \frac{d\underline{k}'^2}{\underline{k}'^2} \left\{ \frac{F(x, \underline{k}'^2) - F(x, \underline{k}^2)}{|\underline{k}'^2 - \underline{k}^2|} + \frac{F(x, \underline{k}^2)}{\sqrt{\underline{k}^4 + 4\underline{k}'^4}} \right\} \\
& \quad - \frac{36\alpha_s^2}{\pi \underline{k}^2 R^2} \frac{N_c^2}{N_c^2 - 1} F^2(x, \underline{k}^2) + \frac{18\alpha_s^2}{\pi \underline{k}^2 R^2} \frac{N_c^2}{N_c^2 - 1} F^2\left(\frac{x}{2}, \underline{k}^2\right), \tag{20}
\end{aligned}$$

where similar to Eq. (13) we define

$$F^{(2)}(x, \underline{k}^2) = \frac{1}{\pi R^2} F^2(x, \underline{k}^2). \tag{21}$$

Eq.(20) is our unitarized BFKL equation for the unintegrated gluon distribution. Since the gluon distribution becomes flatter near the saturation limit, in this range we can take the approximation

$$F\left(\frac{x}{2}, \underline{k}^2\right) \simeq F(x, \underline{k}^2), \tag{22}$$

in Eq.(20), and get

$$\begin{aligned}
& -x \frac{\partial F(x, \underline{k}^2)}{\partial x} \\
= & \frac{\alpha_s N_c \underline{k}^2}{\pi} \int_{\underline{k}'^2_{min}}^{\infty} \frac{d\underline{k}'^2}{\underline{k}'^2} \left\{ \frac{F(x, \underline{k}'^2) - F(x, \underline{k}^2)}{|\underline{k}'^2 - \underline{k}^2|} + \frac{F(x, \underline{k}^2)}{\sqrt{\underline{k}^4 + 4\underline{k}'^4}} \right\} \\
& - \frac{18\alpha_s^2}{\pi \underline{k}^2 R^2} \frac{N_c^2}{N_c^2 - 1} F^2(x, \underline{k}^2). \tag{23}
\end{aligned}$$

3 Numerical analysis

We make some numerical calculations to illustrate the antishadowing effects. For simplicity, we fix the coupling constant to be $\alpha_s = 0.3$. Eq.(20) is the corrections of the gluon recombination to the BFKL evolution equation. Therefore, we use a parameter form of the BFKL solution as the input distribution at $x_0 = 10^{-2}$ [12]

$$F(x_0, \underline{k}^2) = \beta \sqrt{\underline{k}^2} \frac{x_0^{-\lambda_{BFKL}}}{\sqrt{\ln \frac{1}{x_0}}} \exp\left(-\frac{\ln^2(\underline{k}^2/\underline{k}_s^2)}{2\lambda'' \ln(1/x_0)}\right), \quad (24)$$

where $\lambda_{BFKL} = 12\alpha_s/(\pi \ln 2)$ and $\lambda'' \simeq 32.1\alpha_s$. The parameter $\underline{k}_s^2 = 1\text{GeV}^2$ is of nonperturbative origin and the normalization constant $\beta \sim 0.01$. On the other hand, we take $\underline{k}_{min}^2 = 0.01\text{GeV}^2$ in Eq.(20).

We assume that Eq.(20) begins to work from the BFKL-region. In this case, the distribution $F(x_0, \underline{k}^2)$ has a steeper x -dependence at the starting point x_0 of the evolution where the shadowing and antishadowing effects almost cancel out. Thus, we compute the value of $F(x_i/2, \underline{k}^2)$ at the i -th step of the evolution from $F(x_i, \underline{k}^2)$ using the BFKL equation, i.e.,

$$F(x_i, \underline{k}^2) \xrightarrow{\text{BFKL-path}} F\left(\frac{x_i}{2}, \underline{k}^2\right) \equiv F_{BFKL}\left(\frac{x_i}{2}, \underline{k}^2\right). \quad (25)$$

The numerical results show a faster divergence of the distribution $F(x, \underline{k}^2)$ due to the antishadowing effects that cancel out or even outweigh the shadowing effects in the typical BFKL-solution. Of course, we can not expect such infinite growth of the gluons at small x . This unphysical result appears because the BFKL dynamics are not constrained by the energy-momentum conservation, which must be added from the outside of the evolution equation. According to the experiences in the solutions of the modified DGLAP equation, the net antishadowing effects in a small x region always accompany the stronger net

shadowing effects in the smaller x region [11]. One can expect that the evolution asymptotically approaches the BK dynamics under the action of the net shadowing effects. Therefore, we modify the program (25) to

$$F\left(\frac{x_i}{2}, \underline{k}^2\right) = F_{Shadowing}\left(\frac{x_i}{2}, \underline{k}^2\right) + \frac{F_{BFKL}\left(\frac{x_i}{2}, \underline{k}^2\right) - F_{Shadowing}\left(\frac{x_i}{2}, \underline{k}^2\right)}{i\eta^F - \eta^F + 1}, \quad (26)$$

where $F_{Shadowing}(x_i/2, \underline{k}^2)$ indicates that the evolution from x_i to $x_i/2$ is controlled by Eq.(23). The parameter η^F implies the different velocities approaching the BK dynamics. There is a limit value of $\eta_{min}^F \simeq 0.001$ and the solution of Eq.(20) becomes divergent when $\eta^F < \eta_{min}^F$. As an example, we take $\eta^F = \eta_{min}^F$ and divide the evolution into the 100-steps on $|\Delta \log x| = 1$.

In Fig.3(a) we plot the unintegrated gluon distribution function (solid curves) as a function of x for two different values of \underline{k}^2 and where $\eta_{min}^F = 0.001$. The possible solutions of Eq.(20) should lie between the solid and point curves since $\eta^F > \eta_{min}^F$. For comparison, the results of two calculations based on the BFKL equation (dashed curves) and Eq.(23) without the antishadowing effects (point curves) are listed. One can find that Eq.(20) keeps the BFKL-behavior in a larger evolution region than Eq.(23) due to the antishadowing effects.

The \underline{k}^2 -dependence of the unintegrated gluon distribution function with $\eta_{min}^F = 0.001$ is given in Fig.3(b). The saturation of distribution is usually defined as a limit form, which is insensitive to x or \underline{k}^2 . We have not observed such saturation phenomenon in a broad kinematical range, although the obvious suppressions of the net shadowing effects can be found in Fig.3. The reason is that the factor $1/\underline{k}^2$ in both the Eqs.(20) and (23) suppresses the contributions of the nonlinear terms at larger values of \underline{k}^2 .

We give the integrated gluon density using Eq.(3) in Fig.4. We still have not observed the saturation limit on the Q^2 -dependence of the distribution $G(x, Q^2)$ in Fig.4(b). It

is interesting that this conclusion is qualitatively consistent with our previous work [11], where the corrections of the same gluon recombination kernel to the DGLAP evolution equation are considered. Of course, to obtain more practical predictions about the gluon distribution at small x , further corrections should be considered, for example, the corrections from the running α_s , the BFKL dynamics in the IR-region $\underline{k}'^2 \ll 1\text{GeV}^2$, and in particular, the choice of the input distribution. However, the important distinction between the antishadowing effects and shadowing effects as demonstrated in Fig.4 should remain after those corrections are incorporated.

4 Discussions

We try to compare the nonlinear evolution equation (20) with the BK equation, which is originally written in the transverse coordinate space for the scattering amplitude. There are different definitions of the scattering amplitude in the QCD evolution equation. In this work, we note that the BFKL equation for the scattering amplitude $N(\underline{k}^2, x)$ has the following form [13],

$$\begin{aligned}
 & -x \frac{\partial N(\underline{k}^2, x)}{\partial x} \\
 = & \frac{\alpha_s N_c}{\pi} \int_{\underline{k}_{min}^{\prime 2}}^{\infty} \frac{d\underline{k}^{\prime 2}}{\underline{k}^{\prime 2}} \left\{ \frac{\underline{k}^{\prime 2} N(\underline{k}^{\prime 2}, x) - \underline{k}^2 N(\underline{k}^2, x)}{|\underline{k}^{\prime 2} - \underline{k}^2|} + \frac{\underline{k}^2 N(\underline{k}^2, x)}{\sqrt{\underline{k}^4 + 4\underline{k}^{\prime 4}}} \right\}, \quad (27)
 \end{aligned}$$

one can find that $F(x, \underline{k}^2)$ and $N(\underline{k}^2, x)$ differ by a simple scale translation $F(x, \underline{k}^2) \sim \underline{k}^2 N(\underline{k}^2, x)$. Thus, we define the scattering amplitude

$$N(\underline{k}^2, x) \equiv \frac{27\alpha_s}{4\underline{k}^2 R^2} F(x, \underline{k}^2), \quad (28)$$

where we choose such constants on the right-hand side of equation that the following resulting equation is consistent with the BK equation at the saturation limit.

Using Eq.(28) we rewrite Eq.(20) as

$$\begin{aligned}
 & -x \frac{\partial N(\underline{k}^2, x)}{\partial x} \\
 = & \frac{\alpha_s N_c}{\pi} \int_{\underline{k}_{min}^{\prime 2}}^{\infty} \frac{d\underline{k}^{\prime 2}}{\underline{k}^{\prime 2}} \left\{ \frac{\underline{k}^{\prime 2} N(\underline{k}^{\prime 2}, x) - \underline{k}^2 N(\underline{k}^2, x)}{|\underline{k}^{\prime 2} - \underline{k}^2|} + \frac{\underline{k}^2 N(\underline{k}^2, x)}{\sqrt{\underline{k}^4 + 4\underline{k}^{\prime 4}}} \right\} \\
 & - 2 \frac{\alpha_s N_c}{\pi} N^2(\underline{k}^2, x) + \frac{\alpha_s N_c}{\pi} N^2\left(\underline{k}^2, \frac{x}{2}\right). \quad (29)
 \end{aligned}$$

Interestingly, this equation is consistent with the BK equation (in the impact parameter-independent case) in momentum space near the saturation limit due to

$$N\left(\underline{k}^2, \frac{x}{2}\right) \simeq N(\underline{k}^2, x). \quad (30)$$

For the cylindrically symmetric solution, we use the following transformation according to [14]

$$\begin{aligned} N(k, x) &= \int \frac{d^2 \underline{r}}{2\pi} \exp(-i\underline{k} \cdot \underline{r}) \frac{N(r, x)}{r^2} \\ &= \int_0^\infty \frac{dr}{r} J_0(kr) N(r, x), \end{aligned} \quad (31)$$

where J_0 is the Bessel function, one can find that Eq.(29) has the following form in transverse coordinate space

$$\begin{aligned} & -x \frac{\partial N(r_{b0}, x)}{\partial x} \\ &= \frac{\alpha_s N_c}{2\pi^2} \int d^2 \underline{r}_c \frac{r_{b0}^2}{r_{bc}^2 r_{c0}^2} [N(r_{bc}, x) + N(r_{c0}, x) - N(r_{b0}, x) \\ & \quad - 2N(r_{bc}, x)N(r_{c0}, x) + N\left(r_{bc}, \frac{x}{2}\right) N\left(r_{c0}, \frac{x}{2}\right)], \end{aligned} \quad (32)$$

which reduces to the BK equation (in the impact parameter-independent case) at the saturation limit

$$\begin{aligned} & -x \frac{\partial N(r_{b0}, x)}{\partial x} \\ &= \frac{\alpha_s N_c}{2\pi^2} \int d^2 \underline{r}_c \frac{r_{b0}^2}{r_{bc}^2 r_{c0}^2} [N(r_{bc}, x) + N(r_{c0}, x) - N(r_{b0}, x) - N(r_{bc}, x)N(r_{c0}, x)]. \end{aligned} \quad (33)$$

We take the Golec-Biernat-Wüsthoff model [15] as the input amplitude, i.e.,

$$N(r, x_0) = 1 - \exp\left[-\frac{r^2 Q_s'^2}{4}\right], \quad (34)$$

where $Q_s' \simeq 1.4 GeV$ relates to the saturation scale. The computing program of Eq.(32)

is

$$N\left(\underline{k}^2, \frac{x_i}{2}\right) = N_{BK}\left(\underline{k}^2, \frac{x_i}{2}\right) + \frac{N_{BFKL}\left(\underline{k}^2, \frac{x_i}{2}\right) - N_{BK}\left(\underline{k}^2, \frac{x_i}{2}\right)}{i\eta^N - \eta^N + 1}, \quad (35)$$

where $N_{BK}(\underline{k}^2, x_i/2)$ indicates that the evolution from x_i to $x_i/2$ is according to Eq.(33). The minimum parameter $\eta_{min}^N \simeq 0.01$, which is larger than η_{min}^F since the nonlinear effects in Eq.(32) are stronger than that in Eq.(20).

Fig.5 shows the solutions (solid curves) of Eq.(32) with $\eta_{min}^N \simeq 0.01$. For comparison, we give the solutions of the BK equation (point curves) and the linear part of Eq.(32) (dashed curves). The possible solutions of Eq.(32) should lie between the solid and point curves since $\eta^N > \eta_{min}^N$. Fig.6 is such a possible solution with $\eta_N = 0.1$. One can find that the antishadowing effects lead to quite different behaviors between the amplitude $N(r, x)$ and the distribution $F(x, \underline{k}^2)$. The antishadowing effects on the scattering amplitude sharpen the transition form of the amplitude $N(r, x)$ and even violate the unitarity due to $N > 1$ if we take the definition Eq.(28). The reasons for the stronger antishadowing effects are that (1) we use a normalized definition about the amplitude in Eq.(28) so that the coefficients of the nonlinear terms are the same magnitude as that of the linear terms in Eq.(32); (2) the suppression factor $1/\underline{k}^2$ is absorbed by the scattering amplitude due to Eq.(28).

It is interesting that the momentum compensation for the shadowing effects was also discussed using a modified nonlinear evolution equation in Ref.[16]. In the impact parameter-independent case this equation reads

$$-x \frac{\partial N(r_{b0}, x)}{\partial x} = \frac{\alpha_s N_c}{2\pi^2} \int d^2 r_c \frac{r_{b0}^2}{r_{bc}^2 r_{c0}^2} \left\{ 2N(r_{bc}, x) - N(r_{bc}, x)N(r_{c0}, x) - \frac{\partial}{\partial Y} [2N(r_{bc}, x) - N(r_{bc}, x)N(r_{c0}, x)] \right\}, \quad (36)$$

where $Y = \ln(1/x)$ and the last term is the leading order DGLAP corrections. For comparison, we rewrite our Eq.(32) as

$$\begin{aligned}
& -x \frac{\partial N(r_{b0}, x)}{\partial x} \\
& \simeq \frac{\alpha_s N_c}{2\pi^2} \int d^2 r_c \frac{r_{b0}^2}{r_{bc}^2 r_{c0}^2} \left\{ N(r_{bc}, x) + N(r_{c0}, x) - N(r_{b0}, x) - 2N(r_{bc}, x)N(r_{c0}, x) \right. \\
& \quad \left. + N(r_{bc}, x)N(r_{c0}, x) - \frac{x}{2} \frac{\partial}{\partial x} [N(r_{bc}, x)N(r_{c0}, x)] \right\} \\
& = \frac{\alpha_s N_c}{2\pi^2} \int d^2 r_c \frac{r_{b0}^2}{r_{bc}^2 r_{c0}^2} \left\{ N(r_{bc}, x) + N(r_{c0}, x) - N(r_{b0}, x) - N(r_{bc}, x)N(r_{c0}, x) \right. \\
& \quad \left. + \frac{1}{2} \frac{\partial}{\partial Y} [N(r_{bc}, x)N(r_{c0}, x)] \right\}. \tag{37}
\end{aligned}$$

Although Eqs.(36) and (37) have similar nonlinear antishadowing terms (only differ by a factor 1/2), one can find that the main difference between these two equations is that the same momentum compensation mechanism acts on both linear and nonlinear terms in Eq.(36), while the corresponding corrections in Eq.(37) are from the virtual and recombination processes, respectively.

Although we have discussed the contributions of the antishadowing effects to the unitarized BFKL equation, we note, however, that the following problems remain to be solved: (i) As we have emphasized, the replacement of the recombination functions for two BFKL-solutions with $\mathcal{K}_{MD-DGLAP}$ in this work is an approximate method. The unitarized BFKL equation near the saturation range should take a new form ; (ii) How to determine the parameter η^F in Eq.(26)? Perhaps, the most reliable test of the antishadowing effects would be a comparison to the nuclear antishadowing effects, which has been observed in the EMC effect [17]. However, the kinematic region of the nuclear antishadowing effects is about $0.05 < x < 0.3$, where we should combine the DGLAP dynamics in Eq.(20) and it is beyond the scope of the present paper; (iii) The QCD evolution should be performed with running α_s in the numerical procedure. These problems will be our following subjects.

In conclusion, we presented the corrections of the gluon recombination to the BFKL equation and they lead to a new unitarized nonlinear evolution equation, which incorpo-

rates both shadowing and antishadowing effects. The new equation reduces to the BK equation near the saturation limit. The numerical solutions of the equation show that the antishadowing effects have a sizeable influence on the gluon distribution function in the preasymptotic regime.

Acknowledgments: This work was supported by National Natural Science Foundations of China 10135060, 10475028 and 10205004.

References

- [1] G. Altarelli and G. Parisi, Nucl. Phys. B126(1977)298; V.N. Gribov and L.N. Lipatov, Sov. J. Nucl. Phys. 15(1972)438, 675; Yu.L. Dokshitzer, Sov. Phys. JETP. 46(1977)641.
- [2] L.N. Lipatov, Sov. J. Nucl. Phys. 23(1976)338; V. S. Fadin, E.A. Kuraev and L.N. Lipatov, Phys. Lett. B60(1975)50; E.A. Kuraev, L.N. Lipatov and V. S. Fadin, Sov. Phys. JETP 44(1976)443; E.A. Kuraev, L.N. Lipatov and V. S. Fadin, Sov. Phys. JETP 45(1977)199; I. I. Balitsky and L.N. Lipatov, Sov. J. Nucl. Phys. 28(1978)822; I. I. Balitsky and L.N. Lipatov, JETP Lett. 30(1979)355.
- [3] L.V. Gribov, E.M. Levin and M.G. Ryskin, Phys. Rep. 100(1983)1.
- [4] A.H. Mueller and J. Qiu, Nucl. Phys. B268(1986)427.
- [5] I. Balitsky, Nucl. Phys. B463(1996)99; Yu. Kovchegov, Phys. Rev. **D60** (1999) 034008; Phys. Rev. D61(2000)074018.
- [6] W. Zhu, Nucl. Phys. B551(1999)245 .
- [7] V.A. Abramovsky, J.N. Gribov and O.V. Kancheli, Sov. J. Nucl. Phys. 18(1973)593.
- [8] W. Zhu and J.H. Ruan, Nucl. Phys. B559(1999)378; the coefficients of the recombination functions are corrected in W. Zhu and Z.Q. Shen, HEP. & NP. 29(2005)109, hep-ph/0406213.
- [9] W. Zhu, D.L. Xu, K.M. Chai and Z.X. Xu, Phys. Lett. B317(1993)200; W. Zhu, K.M. Chai and B. He, Nucl. Phys. B427(1994) 525; B449(1995)183; W. Zhu, Phys. Lett. B389(1996)374.
- [10] K. Kogut and L. Susskind, Phys. Rev. D9(1974)697; D9(1974)3391.

- [11] W. Zhu, J.H. Ruan, J.F. Yang and Z.Q. Shen, Phys. Rev. D68(2003) 094015.
- [12] A.J.Askew, J.Kwiecinski, A.D.Martin and P.J.Sutton, Phys.Rev. D49(1994) 4402.
- [13] N. Armesto and J.G. Milhano, Phys. Rev. D73(2006)114003; R. Enberg and R. Peschanski, Nucl. Phys. A767(2006)189.
- [14] The Small x Collaboration, J. Andersen et.al., Eur.Phys.J. C35(2004) 67; Anna M. Stasto, Acta Phys.Polon. B35(2004)3069.
- [15] K. Golec-Biernat and M. Wüsthoff, Phys. Rev. D59(1999)014017.
- [16] E. Gotsman, E. Levin, U. Maor and E. Naftali, Nucl. Phys. A750(2005)391.
- [17] M. Arneodo, Phys. Rep. 240(1994)301.

Figure Captions

Fig. 1 The cut diagram containing $4 \rightarrow 2$ gluon recombination kernel (the dashed box) in one step QCD evolution: (a) for the modified DGLAP equation and (b) for the modified BFKL equation, where two legs before fusion are resummed using the DGLAP and BFKL equations in (a) and (b), respectively. The dark area implies the probe.

Fig. 2 The cut diagrams of the gluon recombination kernels for (a) the real processes that yield the antishadowing effects; (b) the interference processes that yield the shadowing effects in the modified DGLAP equation, (c) and (d) are the corresponding virtual diagrams.

Fig. 3 (a) The unintegrated gluon distribution function $F(x, \underline{k}^2)$ as the function of x for different values of \underline{k}^2 . The solid-, point- and dashed-curves are the solutions of Eq.(20) with $\eta_{min}^F = 0.001$, Eq.(23) and BFKL equation, respectively; (b) Similar to (a) but as the function of \underline{k}^2 for different values of x . The possible solutions of Eq.(20) should lie between the solid and point curves.

Fig. 4 Similar to Fig.3 but for the gluon distribution function $G(x, Q^2)$.

Fig. 5 (a) The normalized scattering amplitude $N(r, x)$ as the function of x for different values of r ; (b) Similar to (a) but as the function of r for different values of x . The solid-, point- and dashed-curves are the solutions of Eq.(32) with $\eta_{min}^N = 0.01$, the BK equation (33) and the linear part of Eq.(32), respectively. The possible solutions of Eq.(32) should lie between the solid and point curves.

Fig. 6 A possible solution of Eq.(32) with $\eta^N = 0.1$ (a) as the function of x , and (b) as the function of r .

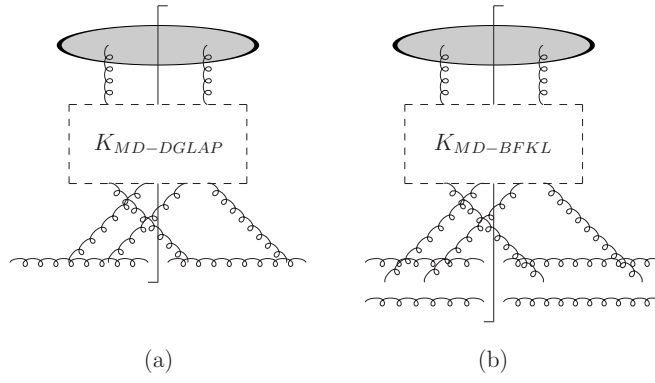


Fig.1

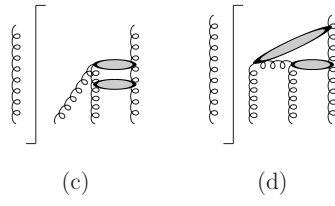
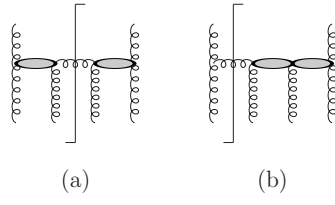


Fig.2

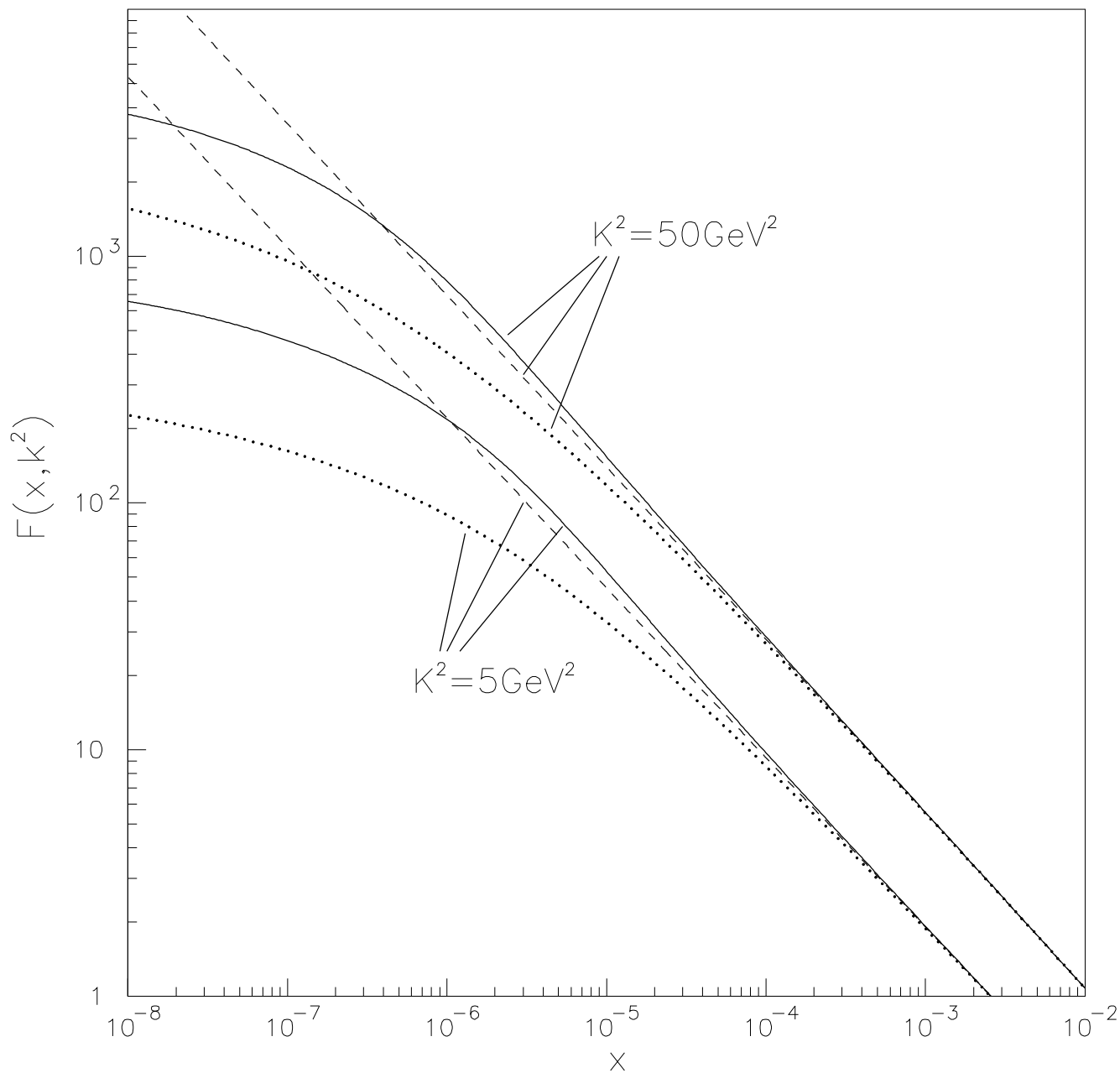


Fig.3(a)

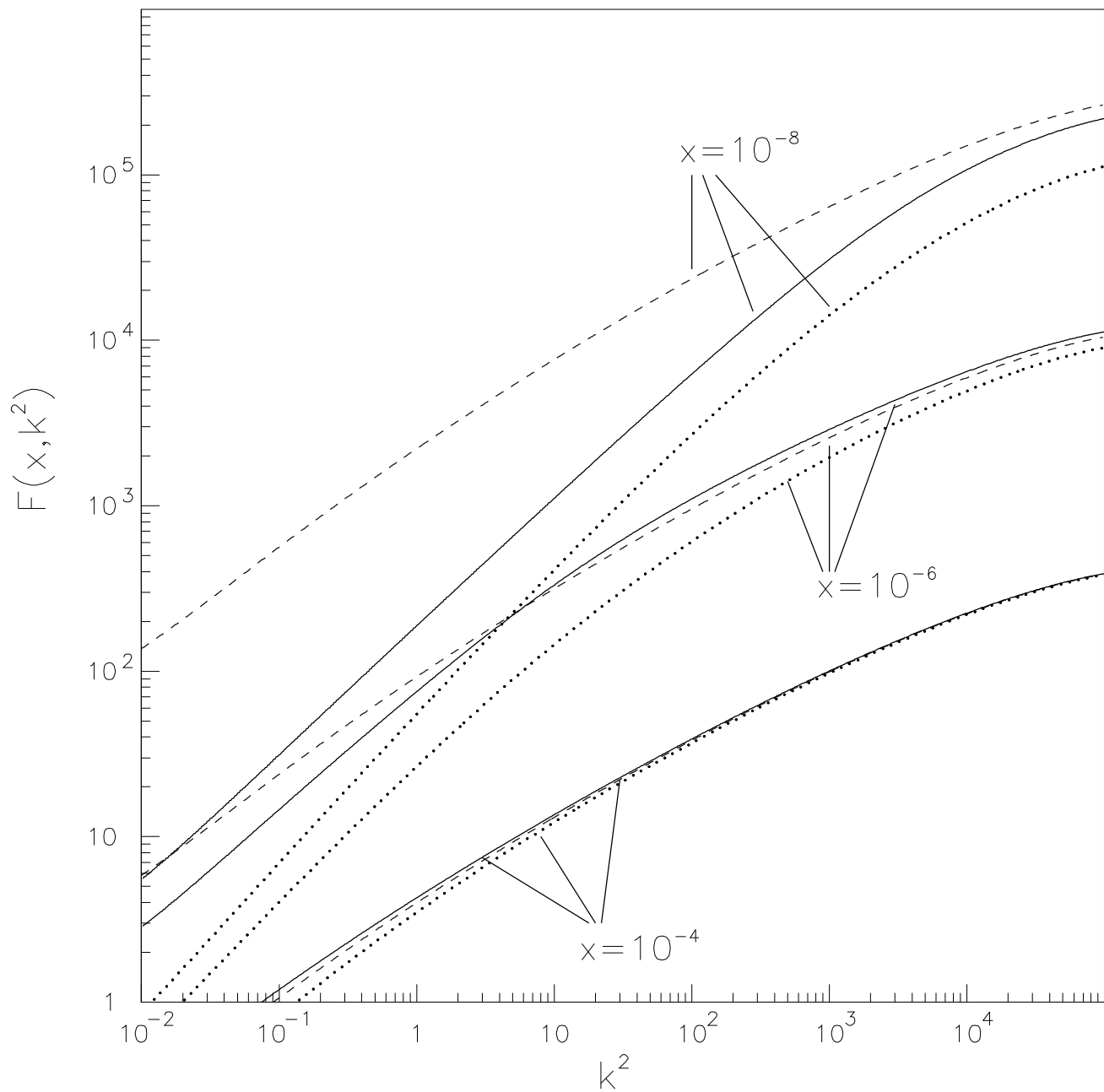


Fig.3(b)

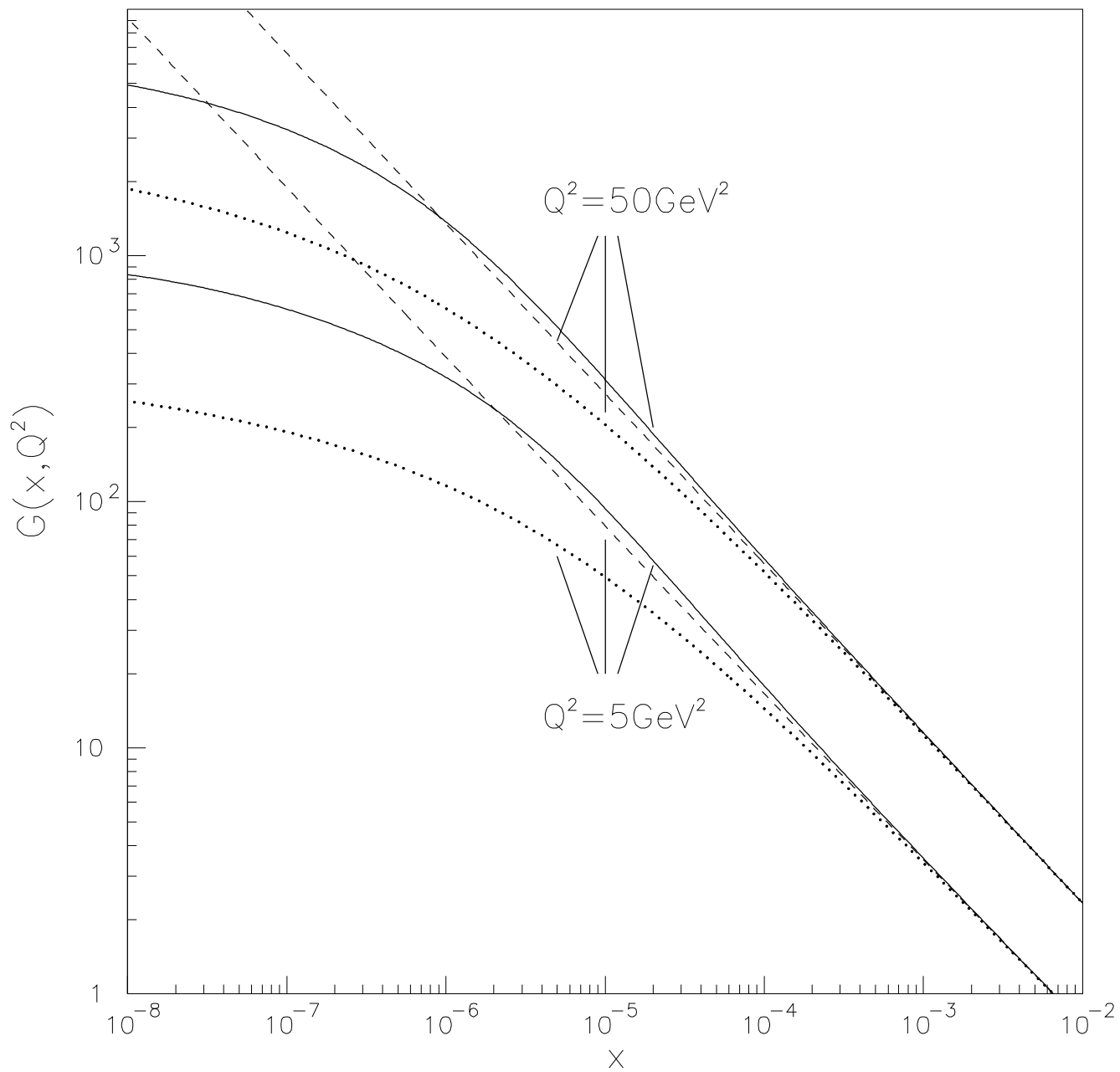


Fig.4(a)

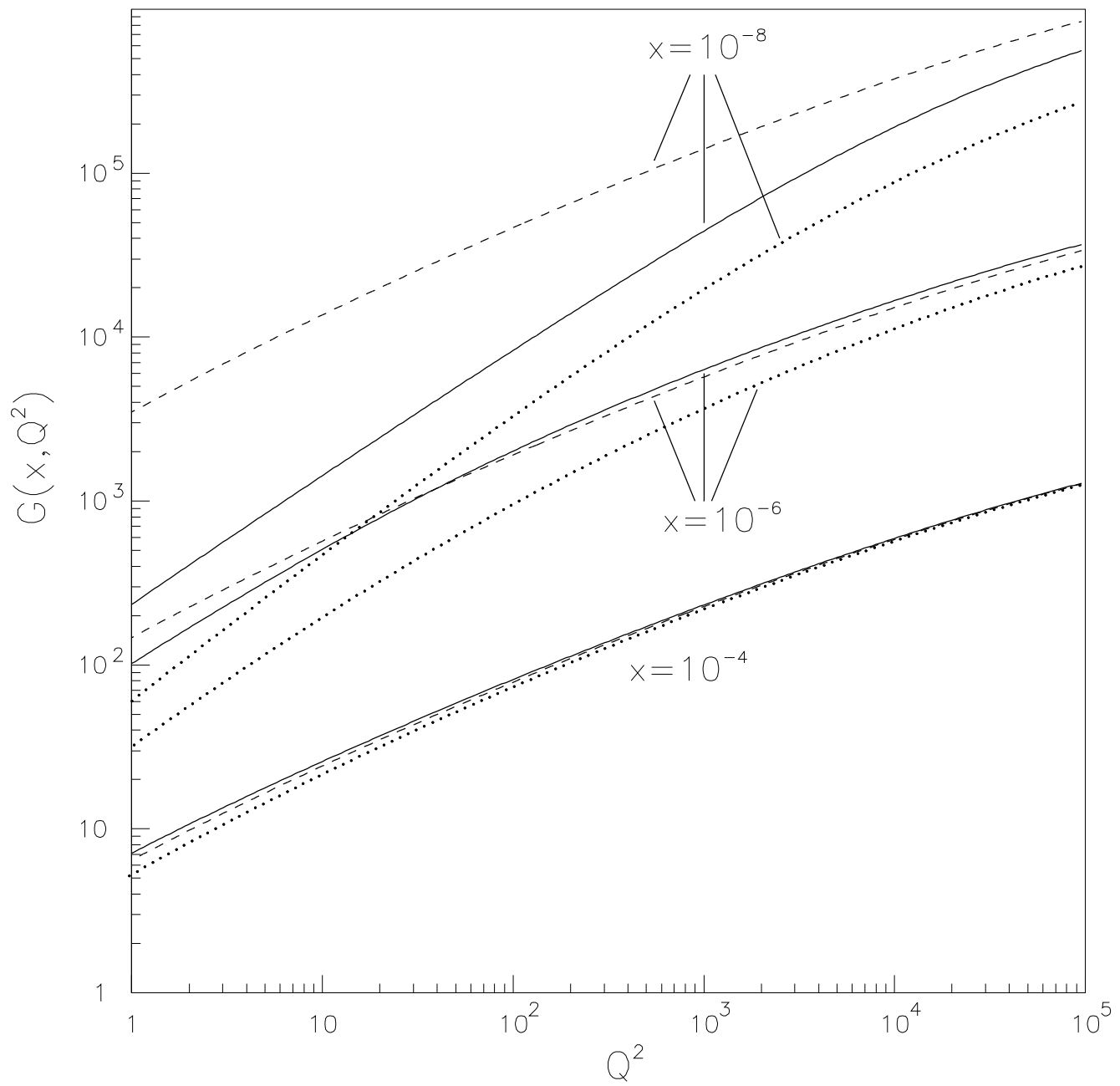


Fig.4(b)

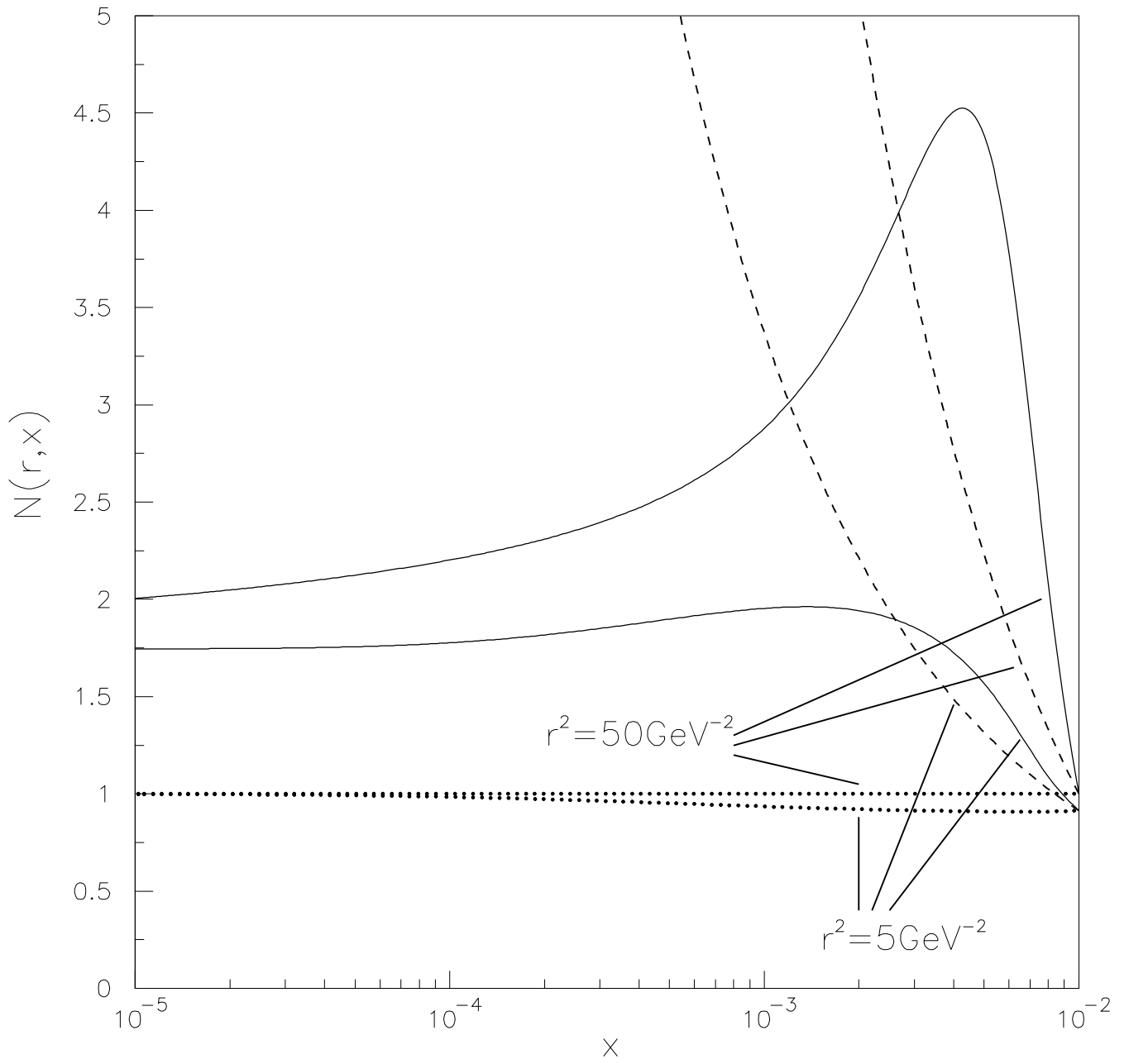


Fig.5(a)

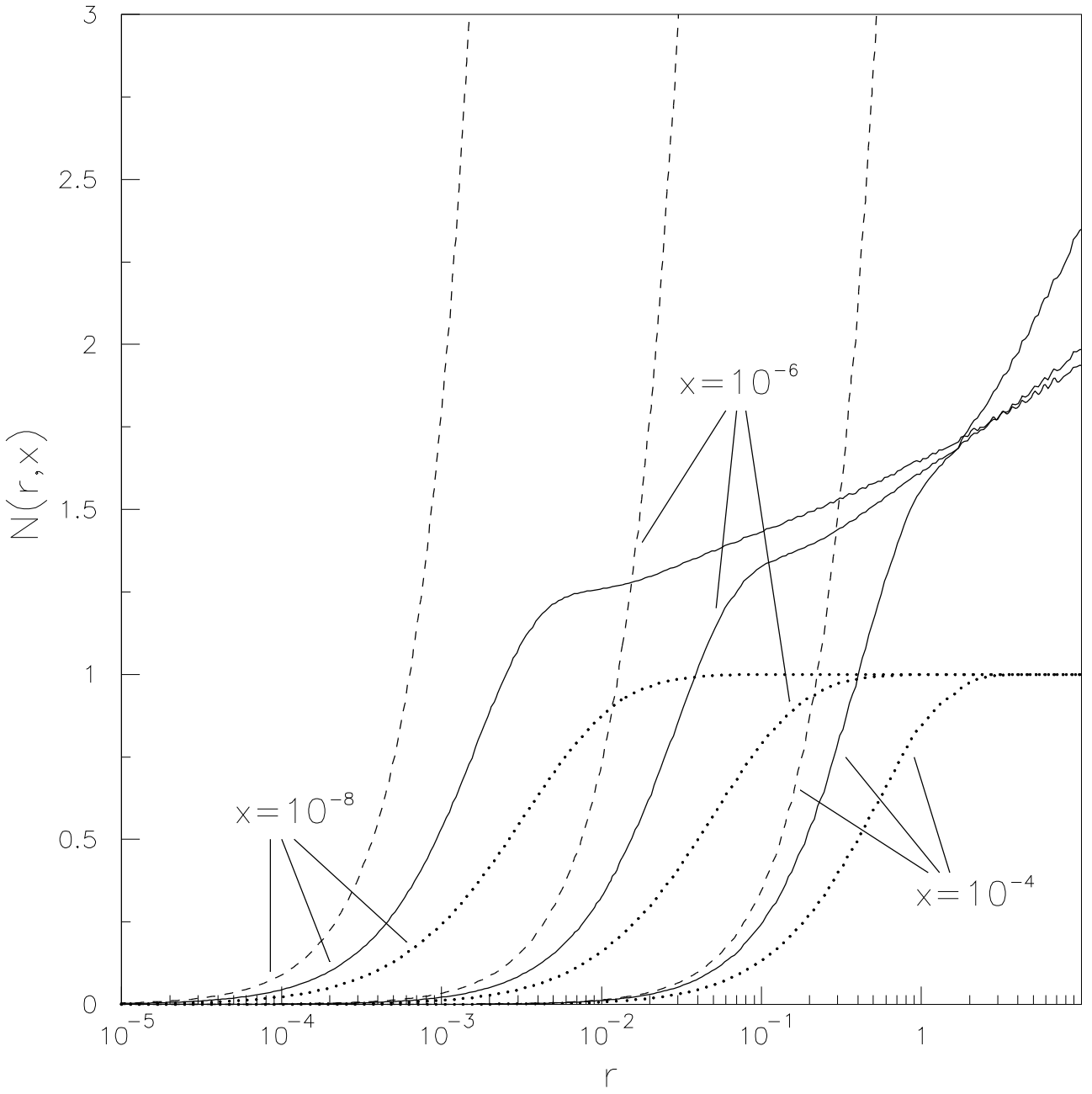


Fig.5(b)

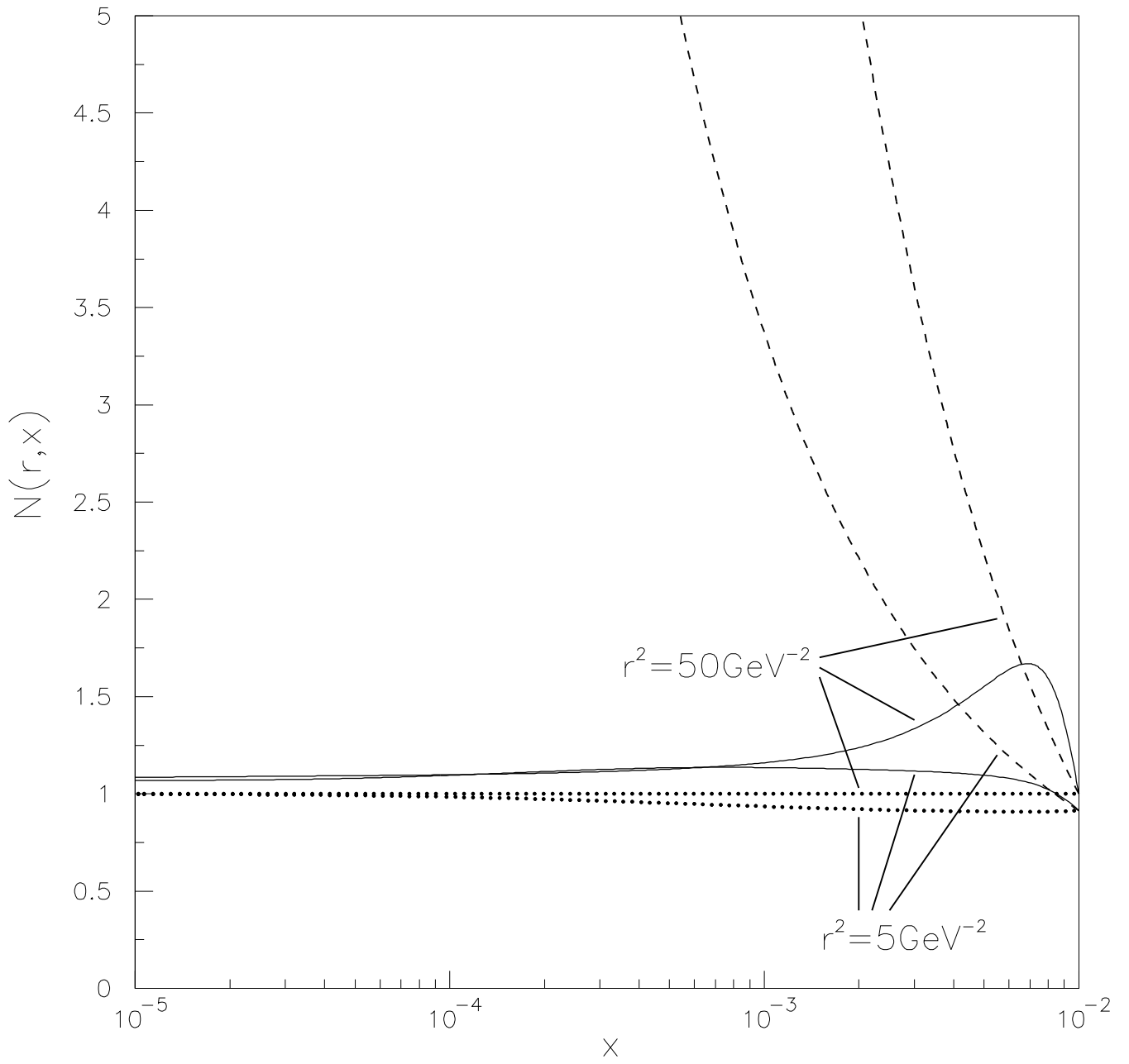


Fig.6(a)

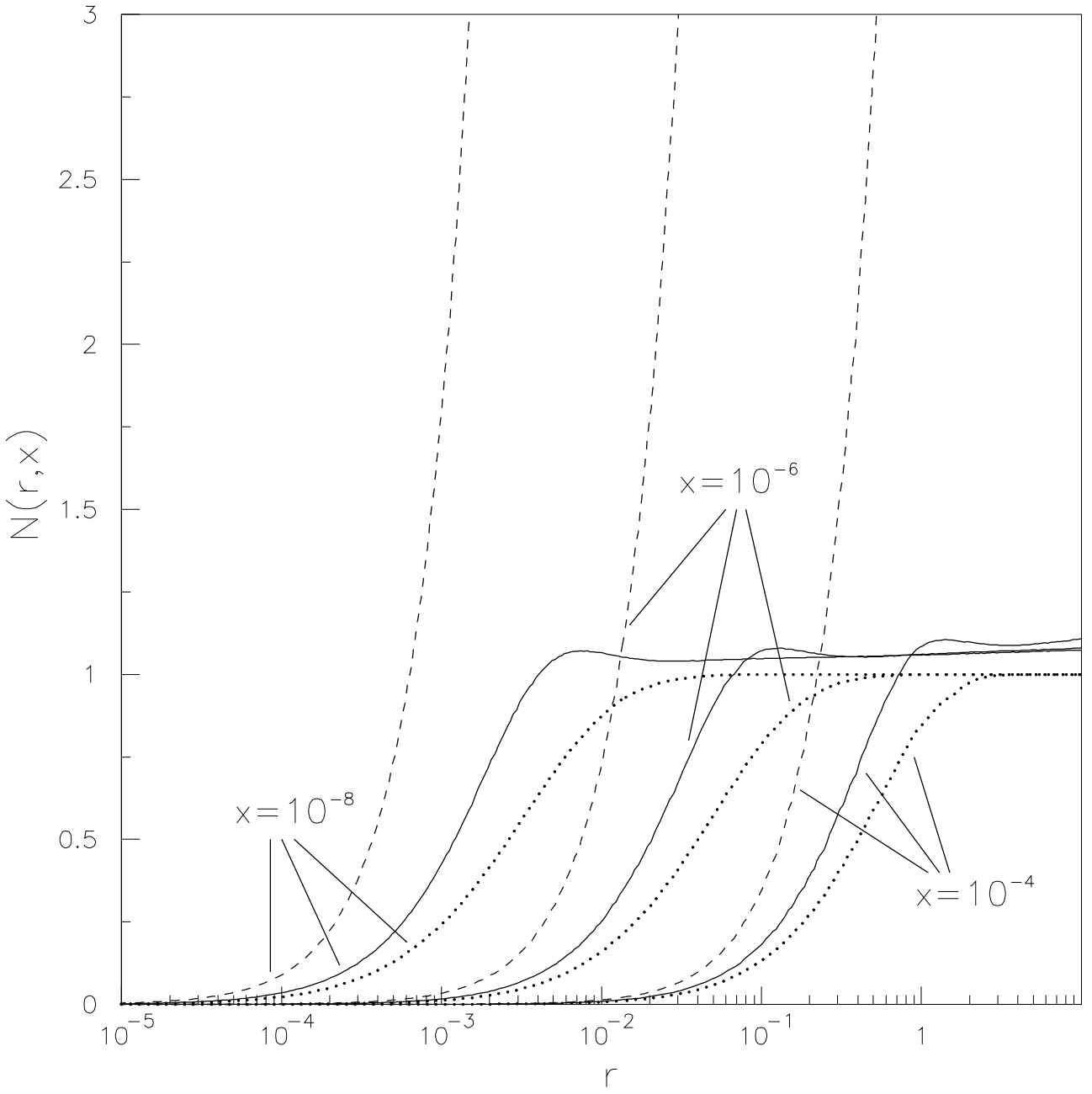


Fig.6(b)